

A. Just · B. Petreska · A. Billard · L. Craighero · A. D'Ausilio · A. Oliynyk · L. Fadiga

Point-to-Point Unconstrained Gestures: Modeling Wrist and Elbow Trajectories

the date of receipt and acceptance should be inserted later

Abstract Although point-to-point reaching motions have received a lot of attention, the way these movements are controlled remains incompletely resolved. Different controllers seem to be recruited depending on the task. Unconstrained reaching movements in space are strongly curved, in opposition to the widely accepted view of quasi-straightness. We argue that the curvature of the movement is due to environmental constraints that affect directly the planning of the movement.

We propose a mathematical model whereby movements are planned through the combination of two concurrent controllers for the wrist and elbow in space. Coherence constraints are enforced between the two systems to simulate biomechanical constraints at the wrist, elbow and shoulder levels. External constraints, such as the presence of obstacles, are encapsulated in a virtual force which affects the planning of the movement.

The predictions of the model are validated against kinematic data from human reaching motions. Four types were contrasted: intransitive versus transitive reaching motions and natural versus un-natural motions. In the un-natural case, subjects were requested to exaggeratedly elevate the elbow during the movement. In all four movements types, the movements are highly curved. The model renders with high accuracy the kinematics of the movements and accounts for the curvature as an effect of the virtual force.

Keywords gesture modeling, VITE model, optimization with Lagrange, unconstrained and voluntary motion, multi-joint arm movement

A. Just · B. Petreska · A. Billard
Learning Algorithms and Systems Laboratory, Ecole Polytechnique Fédérale de Lausanne, 1015 Lausanne. Switzerland

L. Craighero · A. D'Ausilio · A. Oleynik · L. Fadiga
Section of Human Physiology, University of Ferrara, 44100 Ferrara. Italy

L. Fadiga
The Italian Institute of Technology, 16163 Genova. Italy.

1 Introduction

Much attention has been devoted to the study of point-to-point reaching movements, most of which focused on movements restricted to a plane. These studies highlighted several invariant features (Gibet et al 2004), such as quasi-straightness of the hand path from initial and target positions and the so-called bell-shaped velocity profile (Morasso 1981). Soon, such simple rules were questioned when considering unconstrained motions instead of the usual paradigm of constrained motions, or so-called compliant motions (Desmurget et al 1997). Indeed, the majority of the studies of point-to-point movements were highly constrained and required subjects to hold a hand-held cursor. Unconstrained motions, in contrast, refer to free motions of the hand. Results from unconstrained studies show that the spatio-temporal characteristics of compliant and unconstrained movements are fundamentally different. (Desmurget et al 1997) showed that movement duration was higher in the compliant condition than for unconstrained movements. Furthermore, path curvature was significantly higher for unconstrained motions. Hence, compliant and unconstrained motions involve different control strategies. Evidence supports the hypothesis that unconstrained motions are not following a straight line but are slightly curved. This hypothesis is further supported by (Boessenkool et al 1998) who states that trajectory curvature is an inherent property of unconstrained arm movements.

Another largely unresolved issue of motor control relates to the redundancy of the arm joints. A simple way to illustrate this is to consider the various postures that the arm can adopt to touch the same target. Several mathematical models have tried to answer this delicate question. Choosing between describing the kinematics of the arm in Cartesian coordinates or in joint angle space is a thorny problem and evidence comes in support of either of the two representations depending on the task (Flash and Hogan 1985; Rosenbaum et al 1995; Torres and Zipser 2002). To overcome this problem, the

movements are often described more abstractly in terms of a global measure. This measure encodes the cost of each movement and the optimal movement is the one that minimizes this cost function. Cost functions may be defined using either kinematics or dynamic information on the movement.

Cost functions based on kinematic information deal with geometrical and temporal information: position, velocity, acceleration, etc. In (Flash and Hogan 1985), the cost function is defined as the square of the magnitude of the jerk (rate of change of acceleration) integrated over the entire movement. The minimum jerk model generates smooth hand trajectories which are straight and follow a bell-shaped velocity profile.

Cost functions based on dynamic information depend on the forces acting on the hand and arm. The minimum torque change model (Uno et al 1989) proposes as measure of performance the square of the first derivative of the torque integrated over the entire movement. In (Uno et al 1989) the model was compared to the minimum jerk model for unconstrained horizontal movements between two targets located in the sagittal plane. It was shown that the minimum torque change model and minimum jerk model were both predicting straight hand paths. However, for trajectories starting with the arm stretched sideways, the two models gave very different predictions. The minimum jerk model still predicted a straight-line hand paths whereas the trajectories predicted by the minimum torque model were gently curved, and thus more similar to observed human motion.

Other methods have been proposed to model the arm trajectories. Harris and Wolpert proposed the minimum variance theory (Harris and Wolpert 1998). Their model is based on the physiological assumption that the control signal is corrupted by noise. In the presence of this noise, the shape of the hand trajectory is selected so as to minimize the variance of the final arm position. In (Ogihara and Yamazaki 1999), the authors take a very different approach. They modeled the nervous system as a recurrent neural network. Given a goal position, the modeled nervous system was able to generate muscular activation signals used to move the hand to the target position. An interesting feature of this model is its ability to model the position of the whole arm. Most of the models presented previously were dealing mainly with the hand trajectory. A method has been proposed in (Kang et al 2003) to model the arm with its 4 DOFs. The arm trajectory is decomposed into intermediate positions. The model solves the joint angles for these positions by minimizing the sum of absolute value of all joints' torque work in each sub-path (trajectory between two via-positions). Their model unfortunately showed poor results for the adduction/abduction angle of the shoulder. Following this same idea, Gu et al. proposed the equilibrium point based model (Gu and Ballard 2006). The human arm motion can be seen as a sequence of short motion seg-

ments. Movements are generated by gradually shifting from one segment position to the next.

The models we have reviewed in the previous paragraphs are mostly dealing with compliant gestures or are modeling solely the hand path. Few of those have been designed to predict the evolution of movement of the entire arm, from start to target. In the present paper, we propose a method for generating the position of the entire arm for point-to-point motions. Further, since the elbow and hand locations are known, the whole arm configuration is determined, we model the control of the arm trajectory with two concurrent dynamical systems driving the hand and elbow separately, but coupled through kinematics constraints. We extend the biologically plausible VITE model (Bullock and Grossberg 1988), that describes a dynamical system to generate straight point-to-point trajectories in the Cartesian space. The extended VITE model we propose accounts for the observed curvature of the movement. Note that an extension of the VITE model that generate curved writing movements has already been proposed (Bullock et al 1993). The extension consisted in running three coupled VITE controllers to control the x-, y- displacements and wrist rotation of the hand, respectively. The curvature was the result of initiating each model at different starting times. An important disadvantage of this approach to model point-to-point movement is that it required a series of multiple arbitrary targets for each curvature change, which is not the case with the EFF-VITE model.

In order to validate the model, we conduct motion studies, in which unconstrained reaching motions are generated. Most of the literature has focused on the study of reaching movements directed at a target (Atkeson and Hollerbach 1985; Desmurget et al 1997; Magescas and Prablanc 2006). To determine if the curvature of the movement results from generating transitive (i.e. directed to a target) versus intransitive movements, we contrast two conditions in which subjects either reach for an object or do a reaching motion directed to no particular location on a table. We hypothesized that in both conditions the trajectories would be curved and argue that this curvature is necessary and fulfills two main goals: to avoid uncomfortable arm postures (for example, it is more natural to extend the elbow to the right during the motion than keeping a purely straight trajectory) and to encapsulate environmental constraints such as the presence of the table.

Furthermore, in order to better understand how the central nervous system manages to decouple the control of the upper and lower arms, when forced to do so, we investigated the kinematics of motion in which the elbow was forced to follow a trajectory more elevated than that found during natural reaching movements. (Koshland et al 2000) showed that, reaching during movements, the wrist exhibited similar characteristics as the proximal joints, demonstrating a coupling among the joints. We thus expected the curvature of the trajectories of

the wrist also to increase as an effect of the exaggerated elevation of the elbow.

In Section 2 we describe the dynamical systems driving the elbow and wrist motions and explain how coherence constraints between the wrist and elbow are enforced in the model. Section 2.2 describes the experimental set-up and procedure followed during the motion studies. A comparative analysis of the model's predictions and human data is done in Section 3, followed by a discussion of the model's biological plausibility.

2 Materials and Methods

2.1 Description of the model

Our proposed approach is based on an extension of Bullock and Grossberg's Vector Integration To Endpoint (VITE) model (Bullock and Grossberg 1988). The VITE model is a biologically inspired model that can only generate straight point-to-point trajectories. Contrary to the VITE model, the extended force-field version of the VITE model (EFF-VITE) can account for curved reaching movements, and can be used to model both the trajectories of the hand and elbow. Compared to the VITE model, the EFF-VITE model is time-independent and thus stable in case of long lasting perturbations. Furthermore, it represents a proper force governed system. In the EFF-VITE system, the trajectory of the hand or elbow is governed by the following dynamical system:

$$\ddot{x}(t) = \alpha(-\dot{x}(t) + \beta g(t)^\delta (h(t) + \gamma) \left(\frac{x^*(t) - x(t)}{\|x^*(t) - x(t)\|} + g(t)\mathbf{F}(t) \right)) \quad (1)$$

and

$$\mathbf{F}(t) = g(t)\mathbf{u} + h(t)\mathbf{v} \quad (2)$$

where

$$g(t) = \frac{\|x^*(t) - x(t)\|}{\|x(t) - x(0)\| + \|x^*(t) - x(t)\|}$$

$$h(t) = \frac{\|x(t) - x(0)\|}{\|x(t) - x(0)\| + \|x^*(t) - x(t)\|}$$

are respectively the ratios between the distance separating the hand from the final target position x^* and the distance separating the hand from the initial position $x(0)$ over their total. The force \mathbf{F} helps to comply with environmental constraints due to the volume and geometry of the body. \mathbf{F} is the weighted sum of two constant force vectors that push the trajectory away from the straight line. \mathbf{u} is the modulated force that perturbs the beginning of the movement, whereas \mathbf{v} perturbs the end of the movement (Figure 1). The parameter $\alpha \in \mathbb{R}^+$ was fixed to a constant value. Parameters β , γ and δ control the general form of the velocity profile. β controls the

asymmetry and peak value of the velocity profile. γ enables the initiation of the movement, and δ controls the final approaching phase of the movement and parameterizes the trade-off between precision and execution time. For example, lowering the value of δ shortens the movement deceleration phase but also increases the risk of overshooting the target position (Figure 2). The role of the parameters will be further discussed in Sections 3.2.2 and 3.2.3.

An arm configuration corresponds to a particular position in space of both the wrist and elbow. In the duo-EFF-VITE model, two concurrent EFF-VITE models are modeling the hand and elbow paths. As the hand and elbow are linked, these two systems are not independent. Hence, coherence constraints must be enforced in order to have a meaningful representation of the movement. Figure 3 presents the overall structure of the duo-EFF-VITE model. The outcome of the model is the position of the hand and elbow in the Cartesian space at each time step.

Let \mathbf{x}_w and \mathbf{x}_e be the position of the wrist and elbow in the 3D space where the origin is centered on the shoulder. The position of the arm is such that:

$$\|\mathbf{x}_e\| = L_1 \quad (3)$$

and

$$\|\mathbf{x}_e - \mathbf{x}_w\| = L_2 \quad (4)$$

where L_1 and L_2 are respectively the length of the upper arm and forearm, and $\|\cdot\|$ defines the vector norm.

Let $\mathbf{x}_w^d(t)$ and $\mathbf{x}_e^d(t)$ be the desired position of the wrist and elbow given by the EFF-VITE models at each time step t . In general, the variables \mathbf{x}_w^d and \mathbf{x}_e^d will not be consistent with kinematic constraints. In order to have consistent values, we find the values \mathbf{x}_w^* and \mathbf{x}_e^* that minimize the similarity measure H:

$$H(\mathbf{x}_w^*, \mathbf{x}_e^*) = \|\mathbf{x}_w^* - \mathbf{x}_w^d\| + \|\mathbf{x}_e^* - \mathbf{x}_e^d\| \quad (5)$$

under constraints given by equations (3) and (4).

The problem is solved analytically by using Lagrange optimization. We define the Lagrangian as:

$$L(\mathbf{x}_w^*, \mathbf{x}_e^*, \lambda_1, \lambda_2) = H + \lambda_1^T (\|\mathbf{x}_e^*\| - L_1) + \lambda_2^T (\|\mathbf{x}_e^* - \mathbf{x}_w^*\| - L_2) \quad (6)$$

To solve $\nabla L = 0$, we derive respectively $\frac{\partial L}{\partial \mathbf{x}_w^*}$, $\frac{\partial L}{\partial \mathbf{x}_e^*}$:

$$2(\mathbf{x}_w^* - \mathbf{x}_w^d) + \lambda_2 \|\mathbf{x}_e^* - \mathbf{x}_w^*\|^{-1} (\mathbf{x}_w^* - \mathbf{x}_e^*) = 0 \quad (7)$$

$$2(\mathbf{x}_e^* - \mathbf{x}_e^d) + \lambda_1 \|\mathbf{x}_e^*\|^{-1} \mathbf{x}_e^* + \lambda_2 \|\mathbf{x}_e^* - \mathbf{x}_w^*\|^{-1} (\mathbf{x}_e^* - \mathbf{x}_w^*) = 0 \quad (8)$$

We thus need to solve the following system:

$$\begin{cases} 2(\mathbf{x}_w^* - \mathbf{x}_w^d) + \lambda_2 \|\mathbf{x}_e^* - \mathbf{x}_w^*\|^{-1} (\mathbf{x}_w^* - \mathbf{x}_e^*) = 0 \\ 2(\mathbf{x}_e^* - \mathbf{x}_e^d) + \lambda_1 \|\mathbf{x}_e^*\|^{-1} \mathbf{x}_e^* \\ + \lambda_2 \|\mathbf{x}_e^* - \mathbf{x}_w^*\|^{-1} (\mathbf{x}_e^* - \mathbf{x}_w^*) = 0 \\ \|\mathbf{x}_e^*\| - L_1 = 0 \\ \|\mathbf{x}_e^* - \mathbf{x}_w^*\| - L_2 = 0 \end{cases}$$

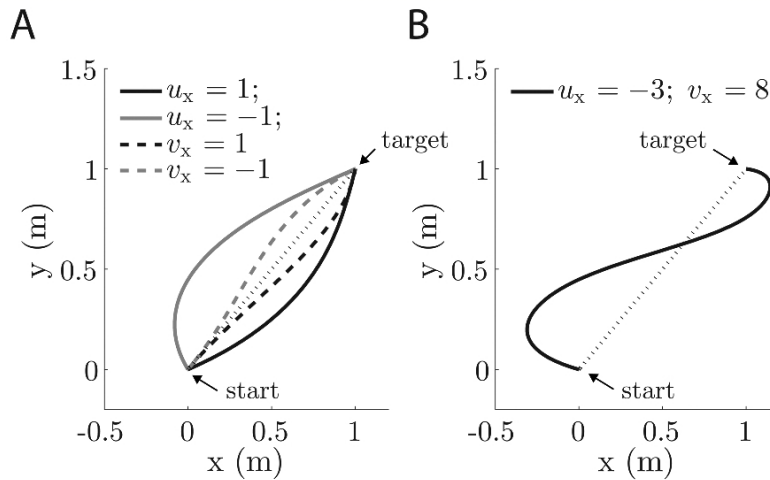


Fig. 1 Dynamics of the movement as a function of the force parameters. A: Forces are modulated such that u affects mostly the beginning of the movement and v mostly the end of the movement. The direction of the deviation from the straight trajectory is determined by the sign of the force. B: By combining the two forces u and v , trajectories that change direction can be obtained. Parameter values: $\alpha = 50$, $\beta = 10$, $\gamma = 0.01$ and $\delta = 1$.

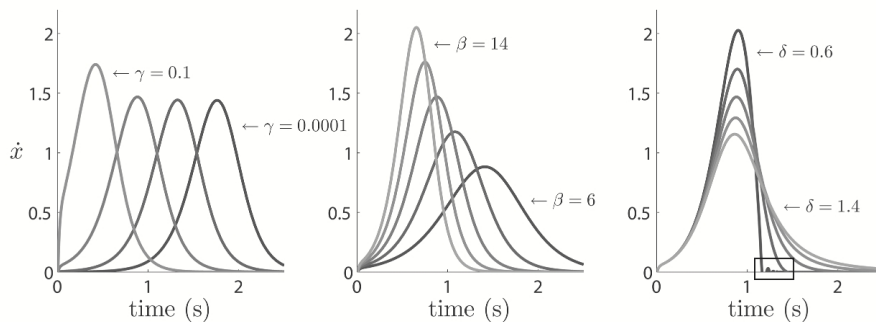


Fig. 2 Effect of the parameters γ , β and δ on the speed profile of the movements. The parameters γ (left) affects the beginning of the movement. The lower its value, the more time it takes the subject to start a movement. β (middle) controls the asymmetry and peak value of the velocity profile (α in our model is constant). δ (right) defined the approaching speed and thus parameterizes the trade-off between precision and execution time. In the rectangle, one can see the arm reaching the target too quickly and overshooting it at $\delta = 0.6$. Parameter values: $\alpha = 50$, $\beta = 10$, $\nu = 1.5$, $\gamma = 0.01$ and $\delta = 1$.

- (9) musculo-skeletal disorder. All had normal or corrected to normal vision.

As the system has several solutions, we choose the solutions \mathbf{x}_w^* , $\mathbf{x}_e^* \in \mathbb{R}$ that minimize H . As the system is non-linear due to the presence of the norm, solutions are found numerically.

2.2 Experiments

Subjects Eight healthy subjects (4 females, 4 males, mean age 26 ± 4) volunteered to perform a one-handed task consisting of point-to-point motions. All subjects were right-handed (Edinburgh Handedness Test, Oldfield (1971)). They were all naive regarding the purpose of the experiment. They reported no history of neurological or

Procedure Subjects sat comfortably on a chair in front of a table. They were asked to maintain a steady trunk position all along the recording session. Each hand movement started in the same rest position, with the forearm lying on the table and perpendicular to the trunk (Figure 4, left). Subjects were shown the movements by a demonstrator. There were two conditions. In the first condition, movements were directed towards an object placed 30 cm away from the subject in the sagittal plane (Figure 4, right). In the second condition, subjects had to reach in front of them and land their hand palm-down on the table. No location on the table was specified in this second condition. We refer to these two conditions

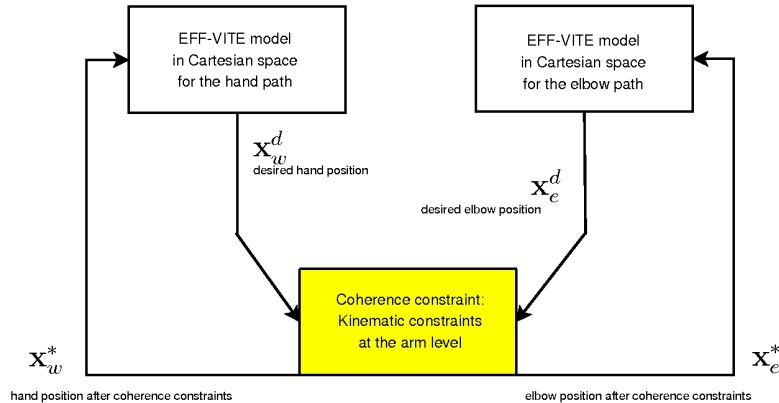


Fig. 3 The wrist-and-elbow path controller: The first EFF-VITE model (on the left) models the trajectory of the wrist in cartesian coordinates, whereas the second EFF-VITE model is used to model the elbow path in cartesian space. The coherence constraints ensure the desired positions \mathbf{x}_w^d and \mathbf{x}_e^d given by the EFF-VITE models are consistent relative to kinematic constraints. The modified values after coherence constraint for both the wrist and elbow positions, \mathbf{x}_w^* and \mathbf{x}_e^* , are fed back to the EFF-VITE models.

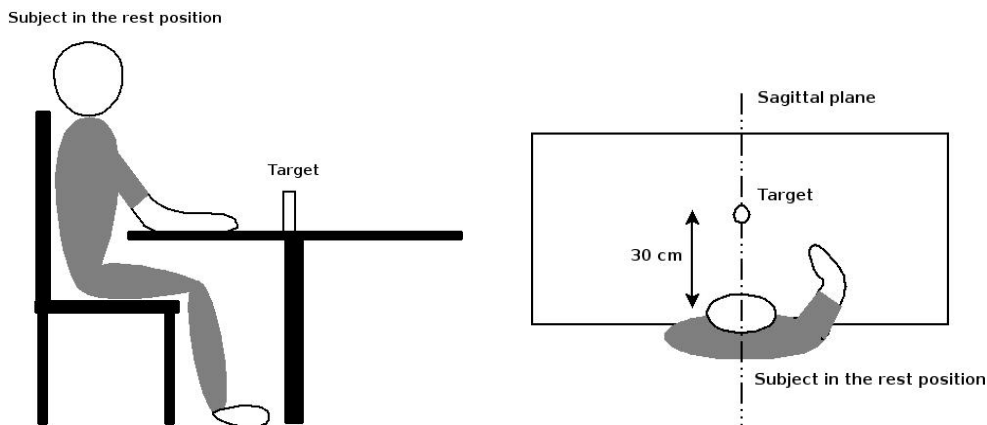


Fig. 4 Left: Experimental set-up seen from the right side with the subject in the rest position. Right: upper view of the set-up showing the position of the target when subjects performed transitive motions.

respectively as transitive (Trans) and intransitive (Intrans) movements in the rest of the paper.

For each condition, the subjects were instructed to perform two variants of the movements. In the first variant (so-called ‘‘Elb’’), the subjects were asked to exaggeratedly elevate the elbow throughout the motion. In the second variant (so-called ‘‘Norm’’), subjects were asked to perform motion in the way that seemed most natural to them. Movements were thus of four types: intransitive with normal kinematics (**Intrans Norm**), intransitive with an exaggerated elevation of the elbow (**Intrans Elb**), transitive with normal kinematics (**Trans Norm**) and transitive with an exaggerated elevation of the elbow (**Trans Elb**). Figure 5 presents snapshots of the four types of reaching movements.

Subjects were shown several times each movement types. Additional explanation was given when necessary. The subjects were instructed to replicate as precisely as

possible these movements. A series of five movements for each condition and variant was recorded for each subject (Table 1).

Data acquisition The trajectory in space of the shoulder, elbow and wrist were recorded by using a kinematics recording system formed by three ProReflex MCU1000 cameras (QUALISYS AB, Sweden) detecting the 3D position of infrared reflecting markers ($n=4$) positioned on the left and right shoulders, right elbow and right wrist. The position of the markers was recorded at a frequency of 200 Hz during the execution of the movements. Figure 6 presents one subject wearing the markers as well as the shoulder-centered frame of reference used in the following of the paper to calculate wrist and elbow trajectories.

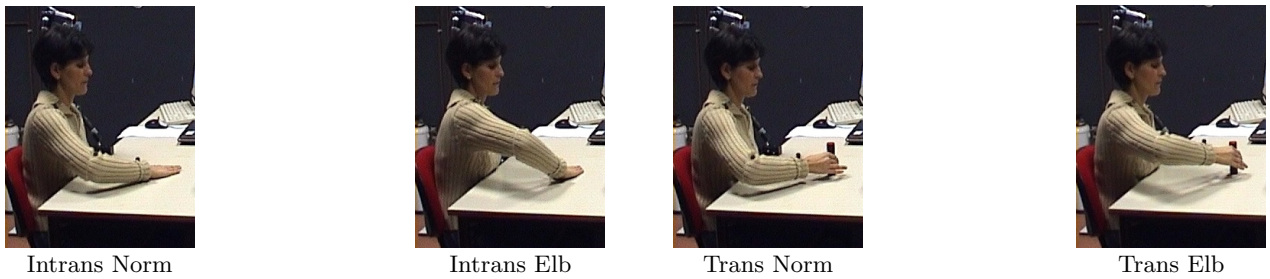


Fig. 5 Snapshots of the four gesture types. From left to right: Intransitive action with normal kinematics and with an exaggerated elevation of the elbow. Transitive movement with normal kinematics and with an exaggerated elevation of the elbow. One can see that for the “Elb” variant the elbow position is always higher than for movements performed with normal kinematics for both the “Intrans” and “Trans” conditions.

Subjects	Repetitions	Recording sessions
8	5×4 gesture types	1

Table 1 Statistics of the database.

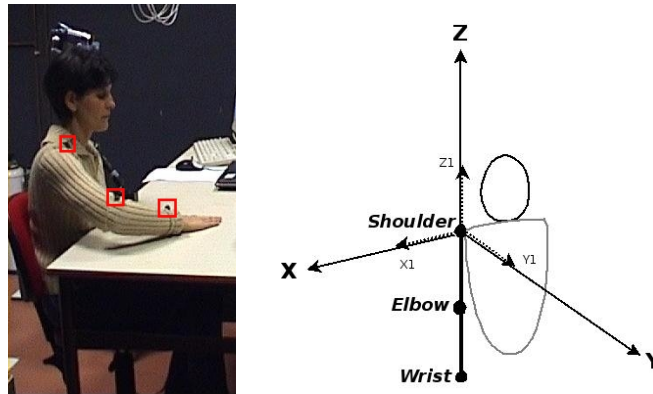


Fig. 6 Left: subject wearing markers on the right arm (markers are surrounded by red squares). Right: shoulder-centered frame of reference.

Data analysis All analyzes were performed using the Qualisys Track Manager (QUALISYS AB, Sweden) software, plus some custom programs written in Matlab (Mathworks, Natick, MA). Analysis was done solely on the reaching phase of each movement (from the rest position to the target location in the case of transitive movements, and from the rest position to the hand placement on the table in front of the subject for intransitive movements). Data were first segmented manually to remove any irrelevant movement prior to the onset of the reaching motion. We used only unfiltered raw values. The curvature index is computed as the ratio between the total arc length of the path and the Euclidian distance between the initial and final positions. A curvature index of 1 indicates a perfectly straight trajectory whereas a semi-circular path would have a curvature index of $CI = \pi/2$. The values of the model’s parameters were optimized for each trial using 5^3 factorial experimental designs coupled with a local search procedure (Neter et al 1996; Hoos and Stützle 2004).

3 Results

3.1 Movement statistics

We first assessed the general characteristics of the recorded movements. For each movement type (Intrans Norm, Intrans Elb, Trans Norm, and Trans Elb), we computed the duration of the movement, path length and curvature index of the wrist and elbow on average across the 8 subjects and 20 trials (Table2).

Consistent with (Bernstein 1967)’s observations of substantial trial-to-trial variations, a three-way ANOVA analysis across subjects (eight levels), conditions (intransitive, transitive) and variants (elbow normal, elbow elevated) revealed a high *inter-subject* variability for both the duration of the movements, the length of the wrist path and the curvature index ($p < 0.001$), with a significant interaction effect for the subject/condition and subject/variant factors ($p < 0.01$ in each case, see Table 2). This high across subjects variability in performing the same motion is illustrated in Figures 7 and 8. Subject 9 tended to be very consistent across trials and

	Duration (s)	Path length (cm)		Curvature index		Elbow elevation (cm)
		Wrist	Elbow	Wrist	Elbow	
Intrans Norm	0.89 ± 0.28	25.3 ± 3.3	26.7 ± 3.5	1.16 ± 0.10	1.19 ± 0.06	-15.0 ± 2.3
Intrans Elb	1.11 ± 0.28	31.8 ± 5.7	37.2 ± 9.6	1.54 ± 0.28	1.52 ± 0.26	-7.0 ± 2.8
Trans Norm	0.84 ± 0.19	22.5 ± 3.0	23.0 ± 3.1	1.16 ± 0.09	1.16 ± 0.05	-15.9 ± 2.0
Trans Elb	1.14 ± 0.22	31.8 ± 6.2	34.9 ± 8.1	1.61 ± 0.45	1.47 ± 0.26	-6.4 ± 2.4
p-value (sub.)	< 0.001	< 0.001	< 0.001	< 0.001	< 0.001	< 0.001
p-value (cond.)	n.s.	< 0.003	< 0.001	n.s.	< 0.02	n.s.
p-value (var.)	< 0.001	< 0.001	< 0.001	< 0.001	< 0.001	< 0.001
p-value (sub*cond)	< 0.001	< 0.001	< 0.001	< 0.001	< 0.002	< 0.001
p-value (sub*var)	< 0.001	< 0.001	< 0.001	< 0.001	< 0.001	< 0.001
p-value (cond*var)	< 0.006	< 0.002	n.s.	n.s.	n.s.	< 0.001

Table 2 Duration, path length, curvature index and elbow elevation across trials and subjects. Three-way ANOVA showed that the movements performed with an exaggerated elevation of the elbow lasted longer, had a longer path for both the wrist and elbow and were significantly more curved than movements with normal kinematics. Furthermore, the recorded movements differed significantly across subjects in their duration, path length, curvature index, and elbow elevation. The maximal height of the elbow during the movement was also significantly different across the two motion variants.

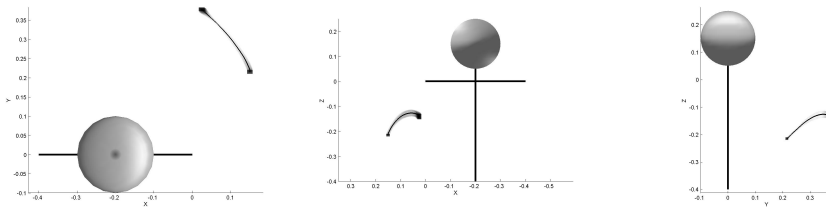


Fig. 7 Mean wrist trajectory (in black) and standard deviation envelope (in grey) for a transitive movement with an abnormal elevation of the elbow (Trans Norm) showing a small intra-variability for Subject 9.

displayed a low across trials variability of the wrist’s motion (Figure 7), whereas Subject 5 displayed an overall much higher variability for the same motion (Figure 8). Given that the subjects had different arm lengths, the length of the wrist path varied importantly across subjects, especially in the intransitive case (see table 2).

All movements were curved ($CI > 1$). Most importantly for the argument of this paper, both the trajectory of the wrist and of the elbow were curved. The curvature is even more important for movements performed with an exaggerated elevation of the elbow ($CI > 1.6$). As a result, movements performed with an abnormal elevation of the elbow in both conditions (Intrans versus Trans) take significantly more time and are longer than movements performed with normal kinematics. Moreover, intransitive motions were significantly longer than transitive motions. This is likely due to the rotation of the wrist that occurs during intransitive motions (to place the palm down on the table), particularly when the movement is performed with an exaggerated elevation of the elbow (first two images in Figure 5).

3.2 Accuracy of the model

We measured the accuracy of the model to reproduce each instance of each motion type. We computed the

mean deviation (MD) of the predicted wrist and elbow trajectories compared to the wrist/elbow trajectories at each time step, as well as the mean squared error (MSE) for each condition and variant of the movements. Table 3 provides these values for each gesture type. We also performed a three-way ANOVA analysis on these results for the subject, condition and variant factors. These results show no significant influence of either factor on the MSE for the wrist. For the elbow, the ANOVA analysis reveals a significant difference between the two motion variants ($F=4.52$, $p < 0.04$). However, the error is small and can be explained by the high variability of movements performed with an exaggerated elevation of the elbow (Elb variant).

Thus, overall, the model reproduces motions with high accuracy. It encapsulates the generic shape of both the trajectory in space and the speed profile of the wrist and elbow (Figure 9). 81% of the data for the wrist and 79% of the observed data for the elbow are reproduced by the model with a MSE inferior to the mean MSE. 3 to 4% of the errors are due to outlier data whereas another 53% are due to a poor reproduction of the start and/or end of the trajectory (Figure 10).

This is due to the fact that, like the original VITE model, the duo-EFF-VITE model, pre-supposes a smooth and gradually increasing and decreasing speed profile at the start and end of the movement, respectively. Because

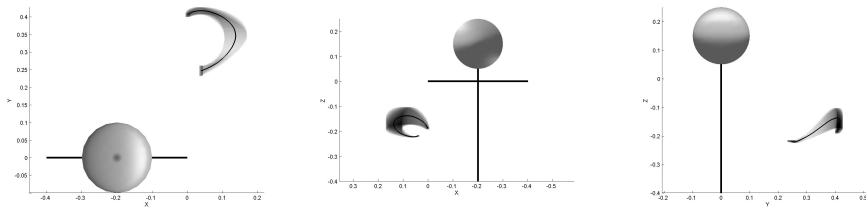


Fig. 8 Mean wrist trajectory (in black) and standard deviation envelope (in grey) for a transitive movement with an abnormal elevation of the elbow (Trans Norm) showing a high intra-variability for Subject 5.

Movement	MD (cm)		MSE (cm ²)	
	Wrist	Elbow	Wrist	Elbow
All motions	1.1 ± 0.7	1.1 ± 0.7	1.26 ± 5.16	1.09 ± 3.23
Intrans Norm	0.9 ± 0.5	0.9 ± 0.4	0.76 ± 1.32	0.65 ± 1.21
Intrans Elb	1.3 ± 0.4	1.3 ± 0.5	1.22 ± 0.86	1.15 ± 1.04
Trans Norm	0.8 ± 0.4	0.7 ± 0.4	0.48 ± 0.86	0.46 ± 1.05
Trans Elb	1.3 ± 1.1	1.4 ± 1.0	2.58 ± 10.10	2.09 ± 6.08
p-value (sub.)	< 0.02	< 0.002	n.s.	n.s.
p-value (cond.)	n.s.	n.s.	n.s.	n.s.
p-value (var.)	< 0.001	< 0.001	n.s.	< 0.04
p-value (sub*cond)	n.s.	n.s.	n.s.	n.s.
p-value (sub*var)	n.s.	n.s.	n.s.	n.s.
p-value (cond*var)	n.s.	n.s.	n.s.	n.s.

Table 3 Mean Deviation (MD) and Mean Squared Error (MSE) for the duo-EFF-VITE models on the trajectories of the wrist and elbow for each gesture type. We also provide three-way ANOVA results across subjects, movement conditions, variants, and interaction of these factors for each error type.

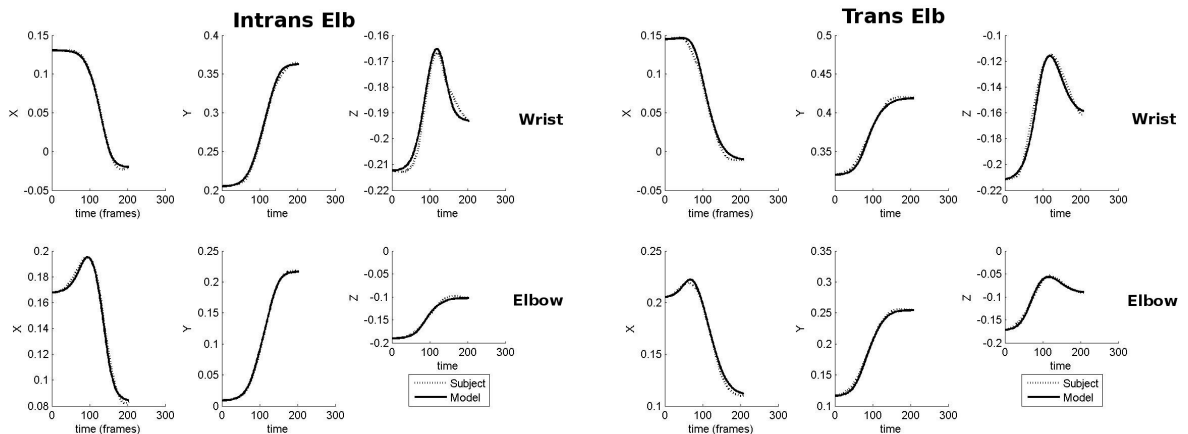


Fig. 9 Examples of movements well reproduced by the duo-EFF-VITE model. The trajectory of the subject's wrist (dotted line) and the modeled trajectory (black) are presented on top.

data were segmented manually, the speed profile was sometimes truncated and hence did not follow the typical pattern. Furthermore, some data present an atypical curvature at the start or end of the movement, due to hesitations on the subjects' parts. Because these imprecisions were minor and did not affect the generic characteristics of each motion (curvature and overall 3D spatial displacement), which we wanted the model to encapsulate, we did not eliminate the data.

3.2.1 Statistics of the model's parameters

A three-way ANOVA across subjects, conditions and variants, on the values taken by the force parameters of the model reveals that, while for the same subject the parameters for the wrist and elbow motions are consistent across conditions and variants, they vary importantly across subjects (see Tables 5 and 6). An effect of the variant (Norm versus Elb) is observed for the parameters

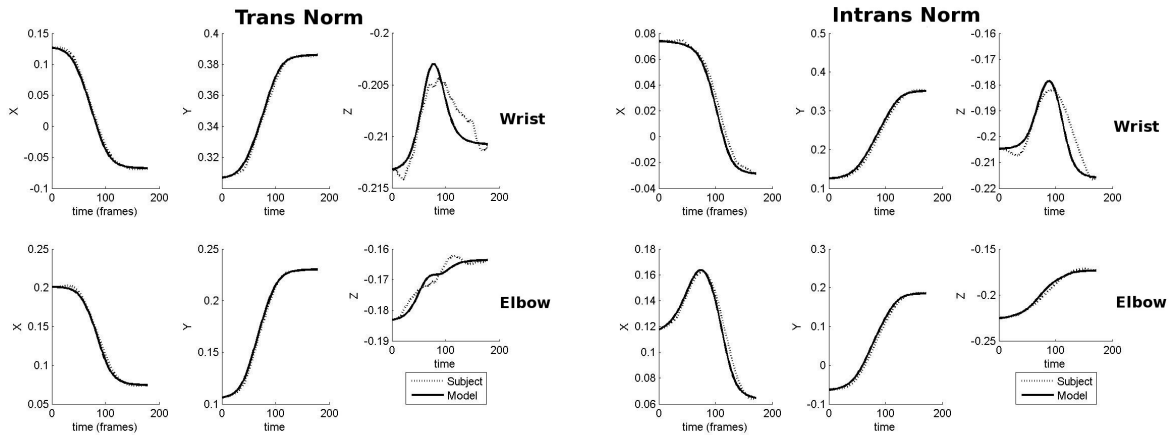


Fig. 10 Examples of movements poorly reproduced by the duo-EFF-VITE model. The trajectory of the subject’s wrist (dotted line) and the modeled trajectory (black) are presented on top.

driving the elbow and this accounts for the variability with which subjects produced the required exaggerated elevation of the elbow (variability is expected given that the arm moved in an unconstrained manner).

We also computed the intra-subject variability of the wrist controller for movements with normal kinematics (Tables 8 and 9). We see that some subjects are more consistent in their movements than others, for both the force applied on the wrist and the parameters modulating the speed profile. This is particularly true for Subjects 6 and 8. This confirms the information contained in Figures 7 and 8, and is consistent with the general observation of a high inter-subject and inter-trial variability when performing the same motion, as discussed above and revealed in Table 2.

3.2.2 Meaning of the model’s parameters

The parameters β , γ and δ in Equation 1 control the velocity profile of the movement. A two-way ANOVA shows that β and γ are similar across conditions and subjects (Table 4 in Annex) for the wrist controller. β controls the asymmetry and peak value of the velocity profile and γ determines the onset of the movements (Figure 2). As any irrelevant movement prior to the onset of the reaching motion has been manually removed, it is expected that γ takes a similar value across subjects and conditions. β is not significantly different across subjects, conditions and variants. Trajectories of the wrist thus follow the same velocity profile for both conditions (Intrans versus Trans) and variants (Norm versus Elb). δ controls the approaching speed of the movement. Together with β , δ determines a trade-off between overshooting the target and minimizing the execution time. Figure 11 presents the distribution of the values for β and δ for all movements. We see that the values are comprised within a region that minimizes execution time while ensuring a good precision of the movement.

3.2.3 Effect of the forces

We have already seen in Table 2 that the trajectories of both the wrist and elbow are curved. This curvature is accounted for by the values taken by the force parameters of the model (Tables 5 and 7). For each condition and variant of the movement, a non-null force is applied on the wrist and elbow. While one could have performed a straight-line motion in the normal condition, it is obvious that a straight path controller could not be envisioned for movements performed with an exaggerated elevation of the elbow. And, as expected, we observed larger values for the force parameters in the Elb variant of the movement.

The force applied along the x and y axes can also be related to the environmental and geometric constraints implied by the task. In our experiments, subjects sat on a chair with the body close to the table, the forearm resting on the table (Figure 6). To perform the movement, subjects needed to avoid the table (“table avoidance” constraint). To satisfy this constraint, the arm had to be placed above the table. Since the elbow is linked to the trunk by the upper-arm, all the possible positions of the elbow are located on a sphere centered on the shoulder and of radius the length of the upper-arm. Thus when the elbow tries to avoid the table, the elbow is also pulled away from the body along the x - and y -directions. Forces applied on the x - and y -axes are thus explained by the geometry of the body as well as the environmental constraints (“table avoidance”).

The force along the z -axis (u_z and v_z) is close to zero in the “Norm” variant. However, in the “Elb” variant, the force along the z -axis at the end of the movement (v_z) (Table 7) is significantly higher ($F=254.3$, $p < 0.001$), with a mean value close to 1, so as to pull the elbow up during the motion. This effect is illustrated in Figures 13 and 12.

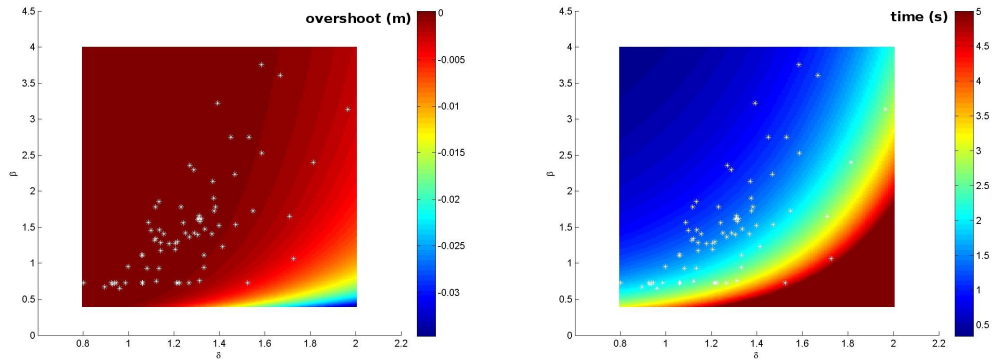


Fig. 11 Distribution of the parameters β and δ of the wrist controller, with respect to the overshoot distance (left) and execution time (right) for a 0.2 m movement. $\alpha = 50$, $\gamma = 0.02$

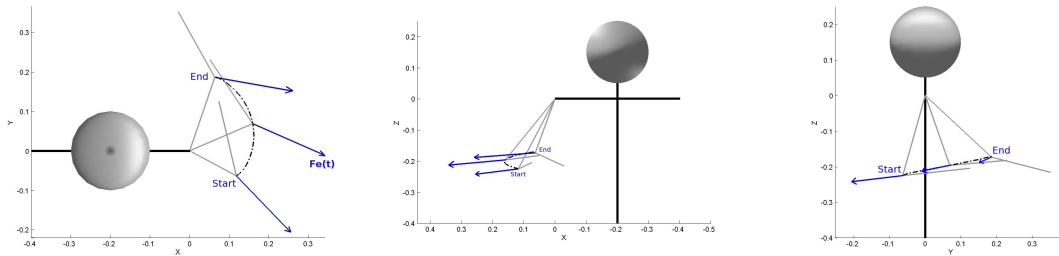


Fig. 12 Example of the force \mathbf{F}_e applied on the elbow for an intransitive movement with normal kinematics. From left to right: projection in the xy -, xz - and yz -planes

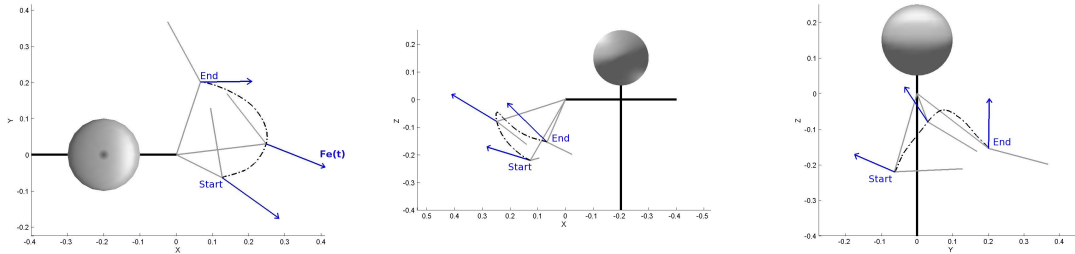


Fig. 13 Example of the force \mathbf{F}_e applied on the elbow for an intransitive movement with an abnormal elevation of the elbow. From left to right: projection in the xy -, xz - and yz -planes

3.2.4 Separate controllers for wrist and elbow

As the elbow and wrist are linked by the forearm, the curvature of the hand path for movements performed with normal or exaggerated elevation of the elbow can be seen as a side effect of the elbow itself. Such correlation is revealed by looking at the Pearson coefficient between the forces ¹ \mathbf{F}_w and \mathbf{F}_e (Equation (2)) applied on the wrist and elbow. These coefficients are respectively:

¹ The Pearson coefficient is the sum of the products of the normalized values of the two measures divided by the degree of freedom. The Pearson coefficient ranges from +1 to -1. If $\rho = 0$, then there is no linear relationship between the two variables. On the contrary, if $|\rho| = 1$, then there is a perfect linear relationship between the two variables.

$\rho(x) = 0.70$, $\rho(y) = 0.74$, and $\rho(z) = 0.18$, where $\rho(x)$, $\rho(y)$, and $\rho(z)$ are the Pearson coefficients along the x -, y - and z -axis, respectively. These results show that there exists a strong correlation between the force applied on the wrist and elbow along the x - and y -axis. The curvature of the wrist trajectories along the x - and y -axis is thus a side-effect of the elbow motion, and would contribute to confirm a view in which elbow and wrist are controlled by a single controller. In contrast, the wrist and elbow seem to be quasi-independent along the z -axis. This indicates that for the Elb variant of the movements, an exaggerated elevation of the elbow results in an increase in the amplitude of the virtual force \mathbf{F}_e along the z -axis of the elbow controller only, and thus speaks in favor of

having two separate controllers for the wrist and elbow, albeit correlated by geometrical constraints.

4 Discussion

4.1 Accuracy of the model

In this paper, we presented a model of reaching movements, which we validated against kinematic data of known motions in two conditions (intransitive versus transitive motions) and for two variants (movements performed with “naturally” versus movements performed with an exaggerated elevation of the elbow). We proposed an extension of the VITE model to account for both the curvature of naturally reaching movements and for the dual control of the wrist and elbow during unnatural reaching movements. The model gave an accurate account of the kinematics of the data for all the four movement types (Intrans Norm, Intrans Elb, Trans Norm and Trans Elb). Discrepancies between the model’s prediction and the data for the velocity profiles at the start and end of the movement were observed in about 10% of the data. Closer analysis revealed that these errors were due to the fact that manual segmentation led to abrupt speed profiles, but also to the fact that in some cases, especially in transitive motions, the speed at the end of the reaching motion was not null (as subjects were transiting directly to a motion in which they grasped and lifted up the object). By construction, the duo-EFF-VITE model, like the VITE model, predicts a zero velocity at target. In effect, when transiting across two motions, subjects tend to displace the target of the reaching motion. One way to simulate this would be to introduce a new target position (corresponding to the final location of the subject’s arm one the object had been lifted) slightly before the hand reached the original target point.

As expected, we observed significant inter-subjects and inter-trials variability across motions. To avoid these, we considered computing and modeling the mean trajectories of the wrist and elbow to capture the nature intrinsic to each movement independently from the subject and trial. This was ruled out as the mean movements of the wrist and elbow could no longer be correlated (since the correlations are not linear). Given that one of the hypotheses of the duo-EFF-VITE model is that the position of the wrist and elbow are controlled via two separate controllers acting in parallel but linked through biomechanical constraints, the effect of these biomechanical constraints would have been lost if we had worked with the mean trajectories. Besides, modeling each motion’s instance allowed us to demonstrate that the curvature at the wrist level cannot be explained without taking into account the movement of the elbow.

4.2 Interpretation of the Model’s Parameters

Parameters of the model are of two types. Three parameters β , γ , and δ are used to modulate the speed profile of the movement. They respectively control the general form of the velocity profile (asymmetry and peak value), enable the initiation of the movement and control the final approaching phase of the movement. Although the model’s parameters were optimized to model each instance of the movements, we observed a consistency across the values of the parameters and showed that the parameter controlling the shape of the speed profile at the end of the movement takes values that optimize a trade-off between the precision and execution time of the whole movement. This is in agreement with the observation of a correlation across speed and accuracy of goal-directed movements (Plamondon and Alimi 1997; Meyer et al 1988). (Meyer et al 1988) hypothesized that this trade-off permits to cope optimally with noise in the human system.

Most importantly, the model hypothesized the existence of virtual forces that encapsulate tasks constraints to modulate a basic controller for reaching movements. We showed that these forces could explain the curvature of the movements of the wrist and elbow and could be interpreted in relation to environmental and biomechanical constraints. Further experiments should be conducted to validate this hypothesis by varying the task constraints, e.g. asking subjects to perform reaching motions by exaggeratedly lowering the elbow, and showing how the forces change as an effect of the context.

4.3 Separate Control of Wrist and Elbow

A second hypothesis inherent to the model is that elbow and wrist are driven by separate controllers, albeit correlated through imagined biomechanical constraints. Such a hypothesis corresponds to assuming that the nervous system is able to plan the mechanical effects that could arise from the motion of the arm segments (Galloway and Koshland 2001). An analysis of the relationship across the forces applied on the wrist and elbow at each time step revealed a strong correlation along the x- and y-axes. The forces along the z-axis were however quasi-independent of the elbow’s elevation. The absence of correlation along the z-direction suggests that the motions of the wrist and elbow are computed separately by the brain. These conclusions are consistent with findings on multi-joint arm movements and with the Leading Joint Hypothesis (LJH) (Dounskaia et al 1998; Dounskaia 2005). The LJH states that there is one leading joint that guides the motion of the entire limb. Muscles of the secondary joints thus just play a regulatory role to ensure that the end-effector performs the required task. Interestingly, the LJH is applicable to our results if we consider the elbow as the leading joint and the wrist as the secondary joint.

4.4 Neural Correlated to the Model's Parameters

Similarly to the VITE model, the duo-EFF-VITE model depends on knowing at all time the wrist and elbow positions and velocities. Evidence that the velocity and position of the wrist may be explicitly computed and used for motor control by the nervous system exists. For instance, cells in the primary motor cortex (M1) of the monkey showed a high correlation between their discharge and the velocity profile of reaching movements (Moran and Schwartz 1999). Moreover (Wang et al 2006) confirmed the existence of a neural representation of the hand location in the motor cortex during reaching. They showed that position and velocity of the hand are simultaneously encoded by cortical motor neurons. Existence that the position and velocity of the elbow are explicitly computed is still questioned (Murphy et al 1982; Scott et al 1997; Reina et al 2001). While the duo-EFF-VITE model proposes a solution to encapsulate environmental and biomechanical constraints, it does not explain how the brain computes such constraints. As they contribute in several ways to the virtual forces, several brain areas may be involved.

Finally, the duo-EFF-VITE model is based on the idea that motions are not planned but unfold through time as the result of the inherent dynamics of the controllers. Such an approach is in line with the force-field approach (Graziano et al 2005), where the target of the motion acts as an attractor for the end-effector. Moreover, the model assumes that control is done in close-loop, taking into account the current position of the arm to correct the motion. This is supported by evidence that the nervous system is able to estimate and anticipate the state of the limb by integrating delayed sensory input and motor output, through afferent and efferent internal feedback loops (Desmurget et al 1997).

While the model exploits a representation of biomechanical constraints in the coupling of the elbow and wrist controllers, it does not account for the way the command are translated into muscle activation of the upper and lower arm limbs. While a complete understanding of the neural control of movements would require a realistic musculoskeletal model², we omitted such complexity in order to focus on explaining the gross dynamics of motor control. In particular, we aimed at explaining how volitional control of one specific limb (upper arm) could be done separately from that of the lower arm, as in the exaggerated elbow elevation condition considered here.

Movements presented in this paper were unconstrained. While this resulted in a high variability across trials and subjects' motions, it offered the opportunity to observe features of motion that are inherent to natural reaching motions. The duo-EFF-VITE model is however generic and could also model constrained movements. To confirm

² Such model is very complex and difficult to obtain due to the numerous muscles and tendons present in the human arm (Cheng and Loeb 2008).

the LJH hypothesis and the use of the duo-EFF-VITE model in support of the latter, it would thus be interesting to replicate the present study with movements of the wrist constrained in the plane. The wrist would then become the leading joint and the elbow the follower. Results of such a comparative study would contribute to explaining the difference in the curvature of the hand path found for constrained and unconstrained movements (Desmurget et al 1997).

Acknowledgements This work was supported by the Sport and Rehabilitation Engineering Program at EPFL, CE Grants Robotcub, CONTACT and Poeticon, and Italian Ministry of University PRIN.

References

- Atkeson C, Hollerbach J (1985) Kinematic features of unrestrained vertical arm movements. *Journal of Neuroscience*
- Bernstein N (1967) The coordination and regulation of movements. Pergamon
- Boessenkool J, Nijhof EJ, Erkelens C (1998) A comparison of curvatures of left and right hand movements in a simple pointing task. *Experimental Brain Research*
- Bullock D, Grossberg S (1988) Neural dynamics of planned arm movements: emergent invariants and speed-accuracy properties during trajectory formation. *Psychological Review*
- Bullock D, Grossberg S, Mannes C (1993) A neural network model for cursive script production. *Biological Cybernetics*
- Cheng E, Loeb G (2008) On the use of musculoskeletal models to interpret motor control strategies from performance data. *Journal of Neural Engineering*
- Desmurget M, Jordan M, Prablanc C, Jeannerod M (1997) Constrained and unconstrained movements involve different control strategies. *The American Physiological Society*
- Dounskaia N (2005) The internal model and the leading joint hypothesis: implications for control of multi-joint movements. *Experimental Brain Research*
- Dounskaia N, Swinnen S, Walter C, Spaepen A, Verschueren S (1998) Hierarchical control of different elbow-wrist coordination patterns. *Experimental Brain Research*
- Flash T, Hogan N (1985) The coordination of arm movements: An experimentally confirmed mathematical model. *The Journal of Neuroscience*
- Galloway J, Koshland G (2001) General coordination of shoulder, elbow and wrist dynamics during multijoint arm movements. *Experimental Brain Research*
- Gibet S, Kamp JF, Poirier F (2004) Gesture analysis: Invariant laws in movement. In: *Gesture-based Communication in Human-Computer Interaction*
- Graziano M, Aflalo T, Cooke D (2005) Arm movements evoked by electrical stimulation in the motor cortex of monkey. *Journal of Neurophysiology*
- Gu X, Ballard D (2006) An equilibrium point based model unifying movement control in humanoids. In: *Robotics: Science and Systems*
- Harris C, Wolpert D (1998) Signal-dependent noise determines motor planning. *Nature*
- Hoos H, Stützle T (2004) Stochastic local search: Foundations and applications. Morgan Kaufmann
- Kang T, Tillery S, He J (2003) Determining natural arm configuration along reaching trajectory. In: *Proc. of the Inter-*

	β	γ	δ
Intrans Norm	2.04 ± 1.94	0.010 ± 0.005	1.31 ± 0.22
Intrans Elb	1.76 ± 1.53	0.006 ± 0.005	1.30 ± 0.37
Trans Norm	2.33 ± 1.75	0.011 ± 0.007	1.43 ± 0.30
Trans Elb	1.61 ± 1.36	0.007 ± 0.004	1.21 ± 0.39
p-value (sub.)	n.s.	n.s.	< 0.001
p-value (cond.)	n.s.	n.s.	n.s.
p-value (var.)	n.s.	< 0.001	< 0.009
p-value (sub*cond)	n.s.	< 0.001	n.s.
p-value (sub*var)	n.s.	n.s.	< 0.008
p-value (cond*var)	n.s.	n.s.	< 0.03

Table 4 Mean and standard deviation for the parameters modulating the speed profile for the movements of the wrist. Three-way ANOVA results for each movement type across subjects, condition and variant have been provided for each of these parameters, as well as interaction effects of the factors.

	u_x	u_y	u_z	v_x	v_y	v_z
Intrans Norm	0.36 ± 0.23	-0.36 ± 0.24	0.18 ± 0.19	0.87 ± 0.71	-0.92 ± 0.65	0.96 ± 0.47
Intrans Elb	0.68 ± 0.30	-0.54 ± 0.34	0.35 ± 0.59	0.32 ± 0.96	-0.24 ± 0.87	1.78 ± 0.60
Trans Norm	0.41 ± 0.26	-0.39 ± 0.26	0.10 ± 0.18	1.28 ± 0.56	-0.88 ± 0.72	0.77 ± 0.51
Trans Elb	0.73 ± 0.60	-0.73 ± 0.45	0.02 ± 0.50	0.71 ± 0.78	-0.14 ± 1.13	1.76 ± 1.00
p-value (sub.)	< 0.001	< 0.001	< 0.001	< 0.001	< 0.001	< 0.001
p-value (cond.)	n.s.	< 0.001	< 0.001	< 0.001	n.s.	n.s.
p-value (var.)	< 0.001	< 0.001	n.s.	< 0.001	< 0.001	< 0.001
p-value (sub*cond)	< 0.001	< 0.005	< 0.03	n.s.	n.s.	< 0.001
p-value (sub*var)	< 0.001	< 0.001	< 0.001	< 0.001	< 0.001	< 0.001
p-value (cond*var)	n.s.	< 0.02	< 0.001	n.s.	n.s.	n.s.

Table 5 Mean and standard deviation for each parameter u and v of the model describing the force at the start and end of the movements of the wrist. Three-way ANOVA results for each movement type across subjects, condition and variant have been provided for each of these parameters, as well as interaction effects of the factors.

	β	γ	δ
Intrans Norm	1.73 ± 0.66	0.011 ± 0.005	1.34 ± 0.14
Intrans Elb	1.55 ± 0.85	0.009 ± 0.004	1.22 ± 0.34
Trans Norm	1.64 ± 0.60	0.011 ± 0.005	1.33 ± 0.18
Trans Elb	1.40 ± 0.79	0.010 ± 0.005	1.27 ± 0.28
p-value (sub.)	< 0.001	< 0.001	< 0.001
p-value (cond.)	n.s.	n.s.	n.s.
p-value (var.)	< 0.03	n.s.	< 0.004
p-value (sub*cond)	n.s.	n.s.	n.s.
p-value (sub*var)	n.s.	< 0.002	< 0.001
p-value (cond*var)	n.s.	n.s.	n.s.

Table 6 Mean and standard deviation for the parameters modulating the speed profile for the movements of the elbow. Three-way ANOVA results for each movement type across subjects, condition and variant have been provided for each of these parameters, as well as interaction effects of the factors.

	u_x	u_y	u_z	v_x	v_y	v_z
Intrans Norm	0.61 ± 0.17	-0.34 ± 0.22	-0.08 ± 0.14	1.50 ± 0.033	-0.59 ± 0.39	-0.09 ± 0.58
Intrans Elb	0.85 ± 0.36	-0.63 ± 0.22	-0.06 ± 0.38	1.48 ± 0.43	-0.25 ± 0.64	1.09 ± 0.93
Trans Norm	0.50 ± 0.11	-0.38 ± 0.23	-0.03 ± 0.17	1.57 ± 0.38	-0.82 ± 0.55	-0.16 ± 0.35
Trans Elb	0.73 ± 0.36	-0.67 ± 0.27	-0.21 ± 0.29	1.44 ± 0.44	-0.56 ± 0.70	1.21 ± 1.05
p-value (sub.)	< 0.001	< 0.001	< 0.001	< 0.001	< 0.001	< 0.001
p-value (cond.)	< 0.001	n.s.	< 0.03	n.s.	< 0.001	n.s.
p-value (var.)	< 0.001	< 0.001	< 0.001	n.s.	< 0.001	< 0.001
p-value (sub*cond)	n.s.	n.s.	n.s.	n.s.	n.s.	n.s.
p-value (sub*var)	< 0.001	< 0.001	< 0.001	< 0.002	< 0.0001	< 0.001
p-value (cond*var)	n.s.	n.s.	< 0.001	n.s.	n.s.	n.s.

Table 7 Mean and standard deviation for each parameter u and v of the model describing the force at the start and end of the movements of the elbow. Three-way ANOVA results for each movement type across subjects, condition and variant have been provided for each of these parameters, as well as interaction effects of the factors.

		u_x	u_y	u_z	v_x	v_y	v_z
Sub. 1	Intrans Norm	-0.07 ± 0.20	0.03 ± 0.13	0.14 ± 0.39	-0.14 ± 0.41	0.11 ± 0.30	0.17 ± 0.45
	Trans Norm	-0.05 ± 0.15	0.02 ± 0.05	0.14 ± 0.39	-0.13 ± 0.40	0.15 ± 0.42	0.16 ± 0.44
Sub. 2	Intrans Norm	-0.05 ± 0.13	0.04 ± 0.13	0.10 ± 0.31	-0.14 ± 0.38	0.15 ± 0.43	0.17 ± 0.44
	Trans Norm	-0.06 ± 0.19	0.04 ± 0.13	0.17 ± 0.46	-0.15 ± 0.44	0.09 ± 0.25	0.16 ± 0.44
Sub. 3	Intrans Norm	-0.07 ± 0.20	0.04 ± 0.11	-0.03 ± 0.11	-0.14 ± 0.45	0.13 ± 0.35	0.17 ± 0.44
	Trans Norm	-0.09 ± 0.25	0.01 ± 0.03	0.05 ± 0.17	-0.11 ± 0.38	0.13 ± 0.35	0.21 ± 0.59
Sub. 4	Intrans Norm	-0.07 ± 0.20	0.03 ± 0.10	0.04 ± 0.17	-0.15 ± 0.42	0.20 ± 0.55	0.16 ± 0.44
	Trans Norm	-0.07 ± 0.20	0.03 ± 0.12	0.10 ± 0.30	-0.13 ± 0.40	0.18 ± 0.50	0.16 ± 0.45
Sub. 5	Intrans Norm	-0.05 ± 0.13	0.01 ± 0.04	0.21 ± 0.55	-0.13 ± 0.35	0.12 ± 0.33	0.17 ± 0.44
	Trans Norm	-0.05 ± 0.14	-0.01 ± 0.04	0.23 ± 0.61	-0.14 ± 0.39	0.04 ± 0.17	0.20 ± 0.54
Sub. 6	Intrans Norm	-0.03 ± 0.09	0.00 ± 0.01	0.14 ± 0.43	-0.12 ± 0.35	0.04 ± 0.13	0.14 ± 0.41
	Trans Norm	-0.02 ± 0.05	0.01 ± 0.03	0.23 ± 0.62	-0.10 ± 0.28	0.05 ± 0.16	0.17 ± 0.45
Sub. 7	Intrans Norm	-0.01 ± 0.08	0.01 ± 0.05	0.12 ± 0.45	0.03 ± 0.26	0.16 ± 0.44	0.20 ± 0.55
	Trans Norm	-0.03 ± 0.11	0.00 ± 0.01	0.18 ± 0.52	0.07 ± 0.21	0.06 ± 0.23	0.20 ± 0.55
Sub. 8	Intrans Norm	-0.01 ± 0.04	0.01 ± 0.04	0.15 ± 0.41	-0.15 ± 0.41	0.04 ± 0.12	0.14 ± 0.38
	Trans Norm	-0.03 ± 0.09	0.01 ± 0.03	0.18 ± 0.49	-0.18 ± 0.48	0.08 ± 0.24	0.16 ± 0.43

Table 8 Mean and standard deviation for each parameter of the model describing the force for Intrans Norm and Trans Norm movements of the wrist for each subject respectively.

		β	γ	δ
Sub. 1	Intrans Norm	0.43 ± 1.60	0.001 ± 0.002	0.04 ± 0.12
	Trans Norm	0.21 ± 0.57	0.002 ± 0.005	0.04 ± 0.12
Sub. 2	Intrans Norm	0.22 ± 0.58	0.002 ± 0.005	0.06 ± 0.17
	Trans Norm	0.36 ± 1.24	0.001 ± 0.003	0.05 ± 0.15
Sub. 3	Intrans Norm	0.25 ± 0.68	0.001 ± 0.004	0.03 ± 0.08
	Trans Norm	0.42 ± 1.46	0.002 ± 0.006	0.03 ± 0.08
Sub. 4	Intrans Norm	0.36 ± 1.57	0.001 ± 0.003	0.03 ± 0.09
	Trans Norm	0.29 ± 1.13	0.001 ± 0.004	0.02 ± 0.08
Sub. 5	Intrans Norm	0.22 ± 0.59	0.001 ± 0.003	0.04 ± 0.12
	Trans Norm	0.32 ± 1.01	0.001 ± 0.002	0.07 ± 0.20
Sub. 6	Intrans Norm	0.15 ± 0.46	0.001 ± 0.004	0.03 ± 0.08
	Trans Norm	0.23 ± 0.64	0.001 ± 0.002	0.04 ± 0.11
Sub. 7	Intrans Norm	0.24 ± 0.94	0.001 ± 0.004	0.10 ± 0.29
	Trans Norm	0.29 ± 0.94	0.002 ± 0.006	0.12 ± 0.31
Sub. 8	Intrans Norm	0.17 ± 0.45	0.001 ± 0.003	0.03 ± 0.09
	Trans Norm	0.21 ± 0.57	0.001 ± 0.003	0.04 ± 0.11

Table 9 Mean and standard deviation for each parameter of the model describing the force for Intrans Norm and Trans Norm movements of the wrist and for each subject respectively.

- national Conference of the IEEE Engineering in Medicine and Biology Society
- Koshland G, Galloway J, Nevoret-Bell C (2000) Control of the wrist in three-joint arm movements to multiple directions in the horizontal plane. *Journal of Neurophysiology*
- Magescas F, Prablanc C (2006) A joint-centered model accounts for movement curvature and spatial variability. *Neuroscience Letters*
- Meyer D, Abrams R, Kornblum S, Wright C, Smith J (1988) Optimality in human motor performance: Ideal control of rapid aimed movements. *Psychological Review*
- Moran D, Schwartz A (1999) Motor cortical representation of speed and direction during reaching. *Journal of Neurophysiology*
- Morasso P (1981) Spatial control of arm movements. *Experimental Brain Research*
- Murphy J, Kwan H, MacKay W, Wong Y (1982) Precentral unit activity correlated with angular components of a compound arm movement. *Brain Research*
- Neter J, Kutner M, Nachtsheim C, Wasserman W (1996) *Applied linear statistical models*. Irwin
- Ogihara N, Yamazaki N (1999) Generation of human reaching movement using a recurrent neural network model. In: *Proc. of the International Conference on Systems, Man, and Cybernetics*
- Oldfield R (1971) The assessment and analysis of handedness: the edinburgh inventory. *Neuropsychologia*
- Plamondon R, Alimi A (1997) Speed/accuracy trade-offs in target-directed movements. *Behavioral and Brain Sciences*
- Reina G, Moran D, Schwartz A (2001) On the relationship between joint angular velocity and motor cortical discharge during reaching. *Journal of Neurophysiology*
- Rosenbaum D, Loukopoulos L, Meulenboek R, Vaughan J, Engelbrecht S (1995) Planning reaches by evaluating stored postures. *Psychological Review*
- Scott S, Sergio L, Kalaskan J (1997) Reaching movements with similar hand paths but different arm orientations. ii. activity of individual cells in dorsal premotor cortex and parietal area 5. *Journal of Neurophysiology*
- Torres E, Zipser D (2002) Reaching to grasp with a multi-jointed arm. i. computational model. *The American Physiological Society*
- Uno Y, Kawato M, Suzuki R (1989) Formation and control of optimal trajectory in human multijoint arm movement. *Biological Cybernetics*

Wang W, Chan S, Heldman D, Moran D (2006) Motor cortical representation of position and velocity during reaching. *Journal of Neurophysiology*